Investigation of the effect of cyanidation after microwave roasting treatment on refractory gold/silver ores by characterization studies

Emine Yoğurtcuoğlu

Faculty of Engineering, Department of Mining Engineering, Niğde Ömer Halisdemir University, Niğde, Turkey

Corresponding author: eyogurtcuoglu@ohu.edu.tr

Abstract: In this article, the efficiency of microwave pretreatment, which is an environmentally friendly, low-energy consuming method for recovery from refractory gold-silver ores, was investigated. The ore sample belonged to the oxidized Bolkardağ deposit, which contains carbonate (calcite, dolomite, smithsonite, hydrozincite), silicate (quartz, hemimorphite), sulfate (beudantite, plumbo-jarosite), and iron oxy/oxyhydroxide (hematite, limonite) minerals. Sulfur/sulfate-bearing silver and gold minerals are found either together with gangue minerals or in inclusions. Approximately 90% gold and 48% silver recovery efficiencies were achieved with the cyanide process after microwave preroasting from the ore. Additionally, the ore, heat treatment product, and waste samples were investigated by characterization studies. In these studies, bond structures, mineral content, sample mass losses, element percentage content differences, and mineral percentage content differences in the samples were determined. As a result, the microwave pretreatment application in cyanidation was presented as a new research topic in terms of its application in the valuable refractory content of this type of oxide.

Keywords: pretreatment, microwave, cyanidation, characterization, refractory gold-silver

1. Introduction

Gold-silver ores can be basically enriched by physical, physicochemical, and chemical methods, as well as their combinations. The way these metals are found in the ore structure is important in determining the methods. Different gravity separators such as shaking tables and multi-gravity separators are used in ores that can be recovered without any chemical effect with the liberation grain size (Clarkson et al., 2016; Burat et al., 2019; Veiga and Gunson, 2020). The flotation process is applied in gold-silver ores found together with minerals such as chalcopyrite, galena, and tetrahedrite, as well as ores requiring pre-oxidation (Faraz et al., 2014; Han et al., 2021). The chemical method is generally carried out with the extraction process and by approximately 90% cyanidation (Cao et al., 2021). Unlike free gold-silver ores (80% < 75 μm grain size > 90% recovery), ores that are not economical to recover by conventional cyanidation methods are called "refractory" ores (La Brooy et al., 1994; Parga et al., 2012). Some of the obvious reasons for the refractoriness of gold-silver minerals in ore content are as follows (Sinadinovic et al., 1999):

- the presence of these ores as inclusions in sulfides, oxides, and silicates,
- finding excess amounts of reactive consuming minerals in the ore,
- ability of the minerals in the ore to adsorb precious metals (preg-robbing),
- the presence of these metals in a crystal lattice structure.

To prevent low recovery yields from refractory Au/Ag ores, the cyanidation process needs to be improved by pretreatment methods. In cases where the reagent cannot reach the particles in the inclusion state, physical pretreatments are applied with ultrafine grinding methods (< 10 μm) such as a stirred ball mill (Aylmore and Jaffer, 2012; Seflek and Bayat, 2018). They are also applied as a biooxidation pretreatment with iron/sulfur-oxidizing bacteria to break down the lattice structures of sulfide minerals (Lorenzo-Tallafigo et al., 2019; Larrabure and Rodríguez-Reyes, 2021). The pressure oxidation method, which is another degradation method that affects the lattice structure of minerals,

is applied under acidic or basic conditions, and it requires advanced technology and high investment costs (Yang et al., 2017). In the chemical pretreatment application before cyanidation, the availability of these metals is increased by decomposing their mineral structures with many different acid/base/salt reagents (Adams, 2005; Kasaini et al., 2008; Li et al., 2009; De Michelis et al., 2013). Thermal pretreatment, which is another one of these pretreatment methods, aims to increase the cyanide contact of gold and silver minerals by separating the sulfur phase in the ore structure under the effect of high temperatures (Dunn and Chamberlain, 1997; Cao et al., 2021).

The microwave pretreatment method, which has recently begun to find an application, also works selectively on ore minerals, similar to these methods (Walkiewicz et al., 1988; Schmuhl et al., 2011). Microwave energy is non-ionizing electromagnetic radiation with frequencies between 300 MHz and 300 GHz and originates from electrical energy with a conversion efficiency of approximately 50% for 2450 MHz and 85% for 915 MHz (Haque, 1999; Zhao et al., 2020; Holmes et al., 2020). Compared to conventional roasting processes, in this process, energy penetrates directly into the material/mineral due to its adsorption at the atomic or molecular level, thus causing a change in the surface of the sample (Jia et al., 2020; Volpi et al., 2022). Therefore, the interior of the material can be hotter than its surface, resulting in a higher heating of samples with poor thermal conductivity (Faraji and Ani, 2014; Li et al., 2020). Since the content of the samples does not generally consist of a single mineral or metal, different minerals in the content have different heating rates, allowing selective processing (Peng and Hwang, 2015; Ai-Yuan et al., 2017). Metal recovery from low-grade ores causes high energy consumption in both pyrometallurgical and hydrometallurgical processes (Kaya et al., 2020). Microwave processing is used in hydrometallurgy for the gradual and selective recovery of various rare earth elements and metals at lower temperatures (Agrawal et al., 2019). This type of ore processing generates high electricity costs as a result of the low conversion effect of electrical energy (Ma and Garbers-Craig, 2006). However, it is advantageous over the conventional roasting processes due to recovery in a shorter time and with higher yields, as is the case with refractory gold ores with high-value or low-tonnage products (Bobicki et al., 2014; Liu et al., 2017; Abo Atia and Spooren, 2020). From the point of view of ore dressing processes, microwave processes have been used in many applications such as drying, carbon reactivation, assisting grinding in many ores, leaching of refractory ores, and cyanide efficiency (Al-Harahsheh et al., 2006; Amankwah and Ofori-Sarpong, 2011; Hartlieb et al., 2016; Forster et al., 2016; Toifl et al., 2017; Forster et al., 2018). Microwave energy has provided very successful results in refractory ores (Li et al., 2021). Although it has been determined that one of the minerals that reached the highest temperatures in this process is Fe_3O_4 at 1258°C, it also reached high temperatures with C (carbon) at approximately 800-1300°C. Common gangue minerals such as quartz, calcite and feldspar (albite-orthoclase) have been discovered to not heat up (Walkiewicz et al., 1988; Kingman and Rowson, 1998; Hunt et al., 2013; Lu et al., 2017). Apart from these, when parameters of 150 W, 5 min and 2450 MHz were applied to jarosite-type minerals, it was concluded that these minerals were transparent or less permeable minerals (Jones et al., 2005; Hassani et al., 2016; Choi et al., 2017).

The sample used in this study was taken from the Niğde-Ulukışla Bolkardağ field and has an oxidized metallic bedding structure. In the ore, in addition to iron oxy/oxyhydroxide structures, carbonate- and sulfate-containing Pb/Zn/Fe structures, jarosite formations, quartz, calcite, and clay minerals are also present. The ore is heavily refractory in terms of gold and silver and contains a small amount of free ore in the form of electrum and native gold. The remaining gold is found in the form of inclusions in gangue minerals or together with these minerals. The silver mineral, on the other hand, is found in the form of acanthite/argentite, jarosite-containing structures (such as argentojarosite), and as inclusions in gangue minerals or the vicinity of these minerals (as in gold mineral) (Mesta et al., 2009). Gold- and silver rich lead concentrates were obtained using the shaking table method for metal recovery. In another study, in which different collectors were tested by flotation, two different concentrates with grades of Au 235-1026 g/t and Ag 3740-10185 g/t were recovered (Acarkan et al., 2011). Gold and silver were acquired at 30-50% and 10-20%, respectively, in the direct cyanidation tests carried out at pH 10.5 at a NaCN concentration of 1.5 g/L for 24 h. Improvements in these metals reached 90-95% Au and 78-90% Ag in the subsequent cyanidation tests of different alkaline pretreatments (Yoğurtcuoğlu, 2017).

Hydrometallurgical processes such as gravity, flotation, and chemical pretreatment were evaluated for this region containing oxidized refractory ore. As also mentioned above, microwave processing is generally considered for sulfide-containing gold ores among refractory ores. In this ore, especially silver is found in the form of acanthite or argentojarosite. The microwave process, which is considered an environmentally friendly and low-energy-consuming method for the refractory structure of sulfide/sulfate-containing silver and gold found together with gang minerals, is evaluated as an innovative study.

In this study, different microwave power values based on a microwave treatment time of six minutes were examined prior to cyanide tests. In addition to gold and silver recovery values, characterization tests were also conducted on the product and the waste sample after the pretreatment. Thus, in addition to metal recovery, it would be appropriate to investigate the changes in the structure in three different samples.

2. Materials and methods

2.1. Materials

This study was carried out using Niğde-Ulukışla Bolkardağ oxidized refractory gold-silver ore. The experiments were performed at Niğde Ömer Halisdemir University Central Research Unit Sample Preparation Laboratories.

Microwave roasting pretreatment experiments were performed with a household microwave. The parameters used in the microwave pretreatment were time (6 min) and microwave power (120-700 kW). The process was started by taking sample weights in microwave-proof containers. At the end of the process, the samples were weighed again. The losses of the samples increased as the power increased, and these values varied between 0.13 and 2.65%. The temperature of the samples was measured with a handheld temperature measurement device from several points on the upper surfaces of the samples. Similarly, these values increased in the range of 55 and 140°C. Since the sample did not consist of a single metal, and thermo-couple measurement could not be made, only the surface measurement result could be determined.

The samples (- 1 mm) used in the experiments were ground after microwave pretreatment. The purpose of grinding after pretreatment is to minimize the possible inclusion effect of the mineral grains from heat treatment. The grinding step was carried out with a Retsch (PM100) planetary ball mill in the Central Research Laboratory. Using 10 balls (5 pieces of 0.5 cm and 5 pieces of 1 cm), the sample was ground for 3 minutes (1.5 min to the right and 1.5 min to the left) in a mill made of tungsten carbide. The particle size distribution of the sample (d_{80}= 31.81 μm) obtained after the milling step is shown in Fig. 1.
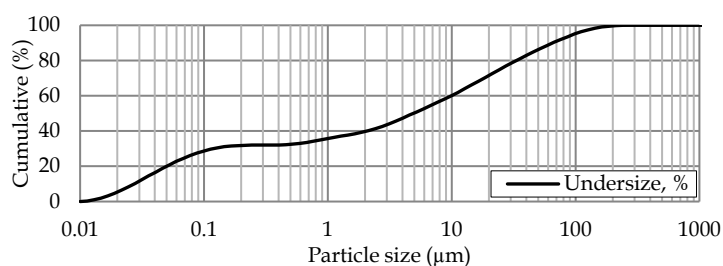

Fig. 1. The particle size distribution of the sample

The results of chemical analysis of the ore are given in Table 1, and the sample contains 24.97% Fe, 22.80% SiO_2, 2.96% Pb and 5.24% Zn. Additionally, the gold and silver grades are determined as 11 g/t Au and 196 g/t Ag.

The samples of the cyanidation experiment were leached for 24 h at a 10% solid ratio and at a NaCN concentration of 1.5 g/L. The pH and cyanide concentrations of each cyanide experiment were controlled at certain intervals throughout the experiment period. These processes were carried out using a magnetic stirrer (750 rpm) under a fume hood. After the cyanidation tests, solid-liquid separation was performed at 2000 rpm at 20°C for 10-15 minutes using the Gyrozen 1580R brand centrifuge device.

Table 1. Chemical analysis of the ore

Element	%	Compound/Element	%	Element	%
Fe	24.97	SiO_2	22.80	Na	0.04
Zn	5.24	Al	2.27	Ba	0.03
Ca	4.32	Mn	1.12	Bi	<0.01
Pb	2.96	K	0.71	Ni	0.009
As	1.58	Cu	0.148	Zr	<0.002
Mg	0.76	TiO_2	0.14	Cd	0.039
S	0.64	P_2O_5	0.05	W	<0.01
Sb	0.05	Cr_2O_3	0.013	Mo	0.006
Sr	<0.01	V_2O_5	0.011	Co	<0.001

2.2. Characterization Analyses

Most of the ore/product/waste characterization studies were carried out at Niğde Ömer Halisdemir University Central Research Laboratories. AAS (atomic absorption spectroscopy) and fire assay analyzes were performed at the Niğde Ulukışla Mineral Processing Facility R&D Laboratories, which belongs to Gümüştaş Madencilik, for Au/Ag analysis only.

The particle size distribution was analyzed on the Malvern Panalytical Mastersizer 3000 device. The measurement value that was found by taking an average of the measurements of 5 samples in the aqueous medium was used in the analyzes.

Chemical analyzes of the raw material sample (percentage of element and compound) were performed with an ACME (Canada) Laboratories device for XRF analysis (X-ray fluorescence) and an ICP-OES (Inductively coupled plasma – optical emission) spectrometer (4 acid digestion method).

The Au/Ag analyzes of the liquid and solid samples were carried out at Tepeköy R&D Laboratories (Gümüştaş Mining-Ulukışla, Niğde). After the fire assay analysis was performed on the solid samples, the precious metals obtained were dissolved, and the liquid samples were analyzed directly in the AAS device. With the cupellation process, 15 g of the sample was first melted at high temperature in a melting pot with slag makers. The molten mixture was poured into steel crucibles and cooled. Then, the slag was separated, the earrings were heated to a certain temperature, and the precious metals (Au/Ag) that were collected in the small bead were analyzed by AAS after the volatilization of the lead was dissolved with aqua regia. XRD (X-ray diffraction) analysis was performed with the Pananalytic brand Empyrean model device at 45 mA and 40 kV at a scanning speed of 2°/min in the range of 5-90. The morphology of the sample was analyzed using a Zeiss EVO40 SEM device (scanning electron microscope) by coating Au for 180 seconds with a current of 20 kV. Additionally, EDS (energy dispersive spectroscopy) analysis was performed from the point determined in the product and waste SEM images. The FT-IR/ATR (Fourier transform infrared spectroscopy/attenuated total reflectance) analysis of the raw material, product and waste samples was performed with a Bruker Vortex 70 spectrometer in the transmittance mode in the wavelength range of 4000-400 cm^{-1}. TGA (thermogravimetric analysis) was carried out with a Linseis STA PT 1600 device to examine the thermal changes of the raw material, the product and the waste samples. The analyzes were carried out in the nitrogen atmosphere in a temperature range of 0-1000 °C with a temperature increase of 10 °C/min.

3. Results and discussion

3.1. Recovery of gold and silver by cyanidation tests after microwave pretreatment

Microwave parameters were determined as microwave time (6 minutes) and microwave power (700-600-460-350-150 W). Cyanide experiments were carried out after each microwave pretreatment. The recovery efficiencies of Au/Ag that were obtained as a result of the cyanidation tests are shown in Fig. 2. The gold recovery efficiencies ranged from 80-90%, and these efficiencies were obtained in the cyanidation tests after applying microwave power values of 350 and 700 W, respectively. Furthermore, the silver recovery efficiency was the lowest at 39% with 600 W power and the highest with cyanidation (48%) after testing with 700 W power, similarly to the case of gold.
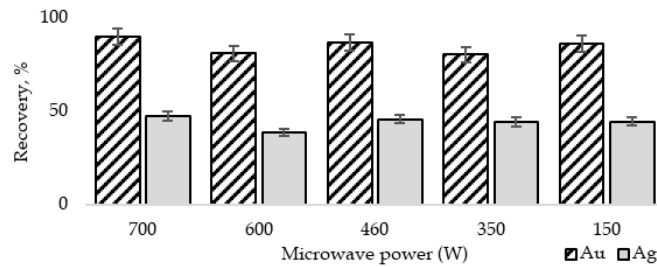
Fig. 2. Recovery of Au and Ag from cyanidation tests after microwave pretreatment (6 min microwave time and microwave power between 120-700 W)

Cyanidation yields of 95% Au and 70% Ag were obtained as a result of a microwave pretreatment in the temperature range of 360-600, and 380°C (sintered with KOH) applied to Au-Ag ores with approximately 15% inclusions in a refractory pyrite-arsenopyrite flotation concentrate (Lunin et al., 1997). Chlorination and subsequent roasting processes applied to cyanidation waste were investigated. Characteristics such as microwave roasting power, energy consumption (1200 W and 78 kJ/g), and the ability to heat the sample quickly are important advantages compared to conventional roasting. A maximum gold recovery of 85.2% was obtained during 15 min of roasting at 1173°C and 1400 W microwave power. In conventional roasting, around 60% gold recovery was achieved at 2700 W (Li et al., 2020). $CaCl_2$ leaching followed by microwave or classical roasting processes was applied to 3 different cyanidation wastes separated into natural gold+bare inclusion, gangue gold and locked gold. As a result of the diagnostic roasting experiments, the recovery was approximately 90% at 900°C. These recovery values were 17.7 times higher, especially in the microwave processes of locked gold (Li et al., 2021).

3.2. Characterization of ore samples

3.2.1. TGA (Thermogravimetric analysis)

According to the results of the TGA of the samples carried out at 0-1000°C, it is seen that mass changes occurred at three different points, 300, 600, and 1000°C. For the raw material sample (Fig. 3), there were mass losses of 6.88, 2.92 (9.80% in total), and 5.56% (15.36% in total) at these temperatures, respectively. In the TGA performed after 6 min of microwave heat pretreatment (product sample) at 700 W, the mass losses were determined as 6.41, 2.75 (9.16% in total), and 5.87%, with a total loss of 15.03%, respectively. The mass losses of the cyanidation test waste sample after 6 min of microwave treatment at 700 W were 5.43, 2.36 (7.78), and 5.65%, with a total reduction of 13.43%, respectively.

In the decomposition of hydrozincite (synthetic), it was observed that water molecules were released at 250-325°C, and CO_2 was released at 325-440°C (Eqs. 1 and 2) (Sinhamahapatra et al., 2012).

In the range of 530-630°C, CO_2 in dolomite minerals is oxidized by decomposing into C and O_2. At 690°C dolomite decomposes into magnesium oxide and calcium oxide, and calcite decomposes into calcium oxide (Nanthakumar et al., 2007; Shahraki et al., 2009). In slurries containing metakaolin, lime, and quartz, calcium silicate hydrate was detected at 60-260°C, while $Ca(OH)_2$ was decomposed at 350-500°C. It turns into a crystal (inversion of quartz) at 573°C (Klimesch and Ray, 1998). Although the

$$C + O_2 = CO_2 \tag{1}$$
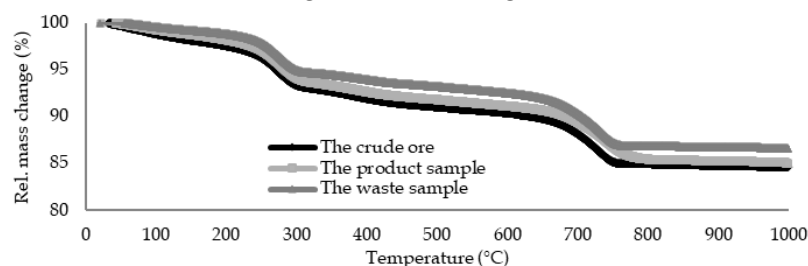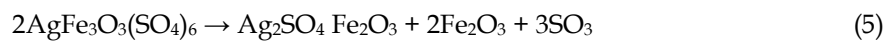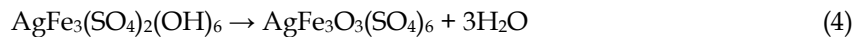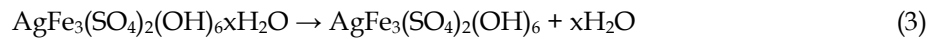
$$CaCO_3 \cdot MgCO_3 = CaO + MgO + 2CO_2 \tag{2}$$

Fig. 3. TGA analysis of the raw material/product/waste sample

thermal degradation processes of lead and silver jarosite differ, they both take place in three basic steps: dehydration, dehydroxylation, and desulfation.

The reactions of all the argentojarosite decomposition steps are as follows (Frost et al., 2010): dehydration at 229°C where the crystallization water is lost, dehydroxylation at 390-435°C where the hydroxyl bond is lost and the water is released, and desulfation at 673-946°C where iron oxide is formed (Eqs. 3-5):

$$AgFe_3(SO_4)_2(OH)_6 xH_2O \rightarrow AgFe_3(SO_4)_2(OH)_6 + xH_2O \tag{3}$$

$$AgFe_3(SO_4)_2(OH)_6 \rightarrow AgFe_3O_3(SO_4)_6 + 3H_2O \tag{4}$$

$$2AgFe_3O_3(SO_4)_6 \rightarrow Ag_2SO_4 Fe_2O_3 + 2Fe_2O_3 + 3SO_3 \tag{5}$$

The possible reason for the initial mass loss change temperature was the separation of water from the ore body. The mass loss at 600°C was thought to be due to the separation of SO_2 from the ore body. Regarding mass loss at 1000°C, there may have been a degradation of O_2, Fe_2O_3 and Pb minerals. Based on the thermal changes of the argentojarosite minerals, it was observed that the H_2O, OH, SO_2/SO_4, O_2 and Fe_2O_3 compounds in the body were affected by thermal pretreatment.

In conclusion, this reduction in the mass loss of the waste sample indicated that the structures in the ore were lost by thermal and chemical processes.

3.2.2.   FT-IR (Fourier-transform infrared spectroscopy)

In the FT-IR analysis of the raw material sample (Fig. 4 a), although the previous peaks could not be determined very well, prominent peaks were observed after 1435 cm^{-1}. Moreover, the stretching vibration of the surface hydroxyl group of kaolinite at 3695 cm^{-1}, the vibration of the inner hydroxyl group of kaolinite at 3618 cm^{-1} (Djomgoue and Njopwouo, 2013) and -CH combinations at 3141 cm^{-1}, 2nd amines (Mogre et al., 2018) were determined. One of the specific peaks of $CaCO_3$ at 1796 cm^{-1} (Kiefer et al., 2018) is associated with the C=O carbonyl group vibrations of the 2nd amide group at 1643 cm^{-1} (Agbozu et al., 2017). It indicates peaks of carbonates such as Na_2CO_3 and $CaCO_3$ at 1435 cm^{-1} (Luo et al., 2011; Kiefer et al., 2018). The O-S-O bond of the Pb-jarosite (Frost et al., 2005) and $CaSO_4 \cdot 0.5H_2O$ peaks (Luo et al., 2010; Kiefer et al., 2018) was observed at 1006 cm^{-1}. Other peaks originated from hydroxyl groups at 909 cm^{-1} (Djomgoue and Njopwouo, 2013), a specific $CaCO_3$ peak at 875 cm^{-1} (Luo et al., 2011; Kiefer et al., 2018), a Si-O-Si bond (such as montmorillonite and quartz mineral) at 797 cm^{-1} (Ojima, 2003; Sbihi et al., 2014), a specific $CaCO_3$ peak at 711 cm^{-1} (Luo et al., 2010; Kiefer et al., 2018), and a $CaSO_4 \cdot 2H_2O$ bond at 665.89 (Kiefer et al., 2018).

The FT-IR results of the heat-treated product (Fig. 4 b) showed peaks similar to those of the raw material sample, and these peaks were 3618-3145-1795-1643-1434-1004-910-875-796-711-664 cm^{-1}. Apart from this, 2350 and 2325 cm^{-1} peaks demonstrate the presence of CO_2 (Chuprov et al., 2006; Kauffman et al., 2011). A peak of 2114 cm^{-1} suggests the presence of the C≡N group (Miletto et al., 2018) and the presence of CO (Idriss and Llorca, 2019). A peak of 1162 cm^{-1} indicates the C-N aromatic group (Sanches et al., 2015). A peak of 672 cm^{-1} can be associated with the Fe-O stretching vibration of Fe_3O_4 (Abdolmohammad-Zadeh and Salmasi, 2018). A peak of 516 and 455 cm^{-1} shows O-C-O bonds (Subhan et al., 2014) and Si-O vibrations (Jabeen and Rafique, 2014), respectively.

Similarly to the raw material sample, the FT-IR peaks in the waste sample (Fig. 4 c) obtained after cyanide treatment included the 3696, 3618, 1791, 1643, 1434, 1003, 907, 874, 795, 711 cm^{-1} peaks. There were also 2350, 2325, 2113, 1162, 672 and 452 cm^{-1} peaks similar to the heat-treated sample. Unlike both samples, other peaks indicated a CH bond at 3116 cm^{-1} (Zhang et al., 2019), cyanide ions at 1988 cm^{-1} (El-Nafaty et al., 2013), a C-O-C bond at 1076 cm^{-1} (Zhang et al., 2019), an O-Si-O bond at 692 cm^{-1} (Šontevska et al., 2008), and the Si-O deformation of kaolinite at 433 cm^{-1} (Kumar and Rajkumar, 2009). As a result, gangue minerals such as calcite, quartz, and kaolinite were determined in the FT-IR analysis. Additionally, cyanide bonds were revealed in the waste sample after cyanidation.

3.2.3. SEM/EDX (Scanning electron microscopy/Energy dispersive X-Ray) analysis

In the SEM/BSE (backscattered electrons in scanning electron microscopy) imaging analyses performed on similar samples, gold and silver were determined as native gold, electrum, jarosite, and

acanthite. Their occurrence in the ore was determined as inclusions or together with clay, quartz, calcite, Fe oxy/oxyhydroxide, and sulfate-arsenate structures (Yoğurtcuoğlu, 2017).

In this study, SEM images were obtained from the sample taken from the raw material sample. Fig. 5 shows carbonate-structured minerals (about 90 µm) containing many large and small particles found in the ore.
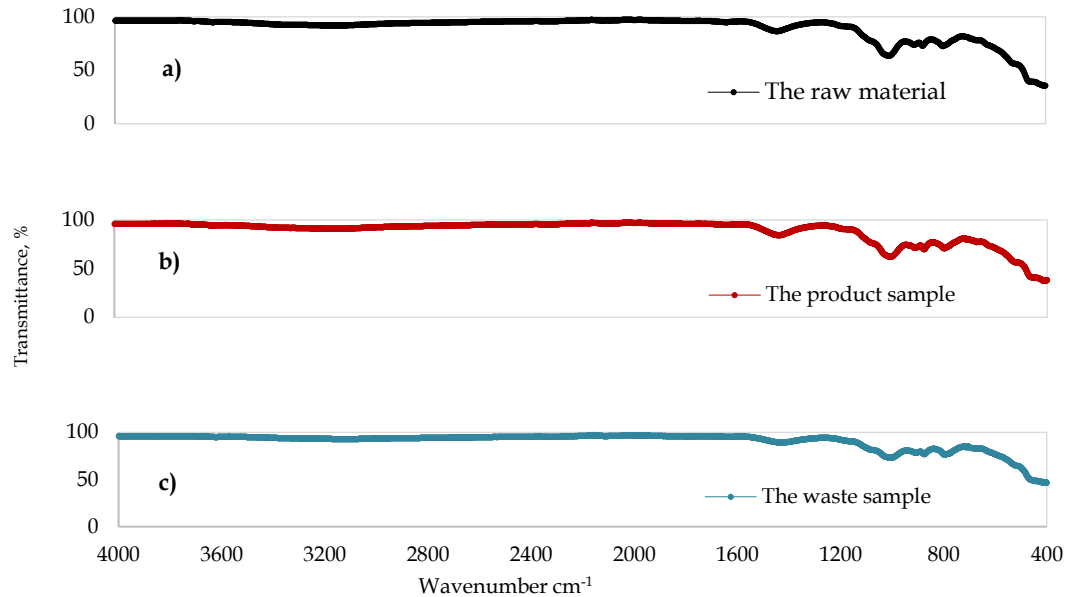

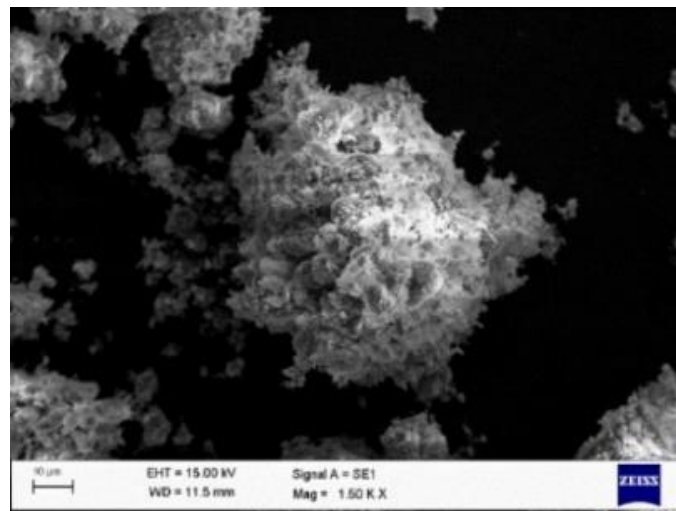Fig. 4. The FT-IR analysis of the raw material/product/waste sample

Fig. 5. Carbonate-containing mineral determined in the SEM analysis of the raw material sample

The EDX (Energy-dispersive X-Ray) spectra of the samples were analyzed from the region marked in the SEM microstructure image taken on the product obtained after microwave pretreatment (Fig. 6 a). Based on the elements detected in the EDX analysis of the marked area (Fig. 6 b), the structure was indicated to be metal carbonate (with Pb/Fe/Ca carbonate structure) and a mineral containing SiO_2 such as a small amount of quartz.

EDX analysis was performed on the waste sample of the cyanidation test (Fig. 7 a) after microwave treatment, from the area determined on the SEM image, as in the product. The elements determined in the EDX analysis of the marked area (Fig. 7 b) suggested the presence of mineral structures of iron oxy/oxyhydroxides (e.g., hematite, goethite), silicates (e.g., kaolinite, feldspar, hemimorphite), and carbonates (e.g., calcite, dolomite).

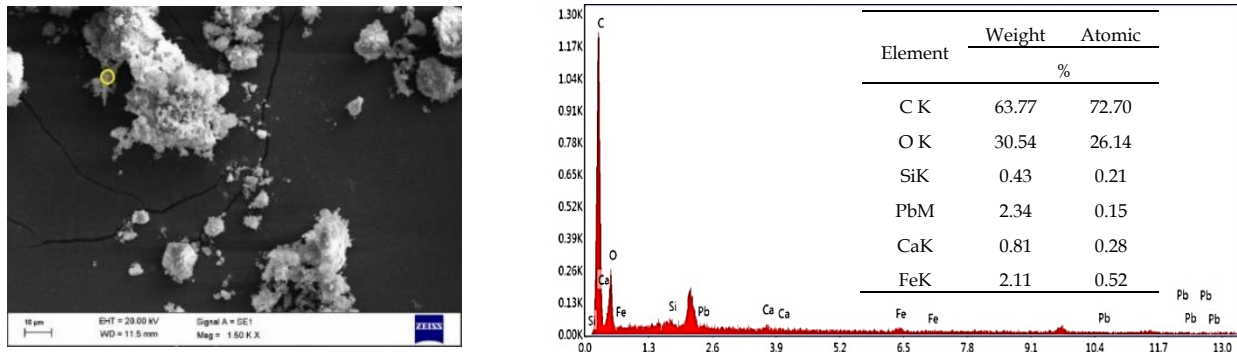| Element	Weight	Atomic
		%
C K	63.77	72.70
O K	30.54	26.14
SiK	0.43	0.21
PbM	2.34	0.15
CaK	0.81	0.28
FeK	2.11	0.52

Fig. 6. a) SEM analysis of the sample after heat pretreatment (left-fig.); b) EDX analysis of the marked area in the SEM image of the product sample (right-fig.)

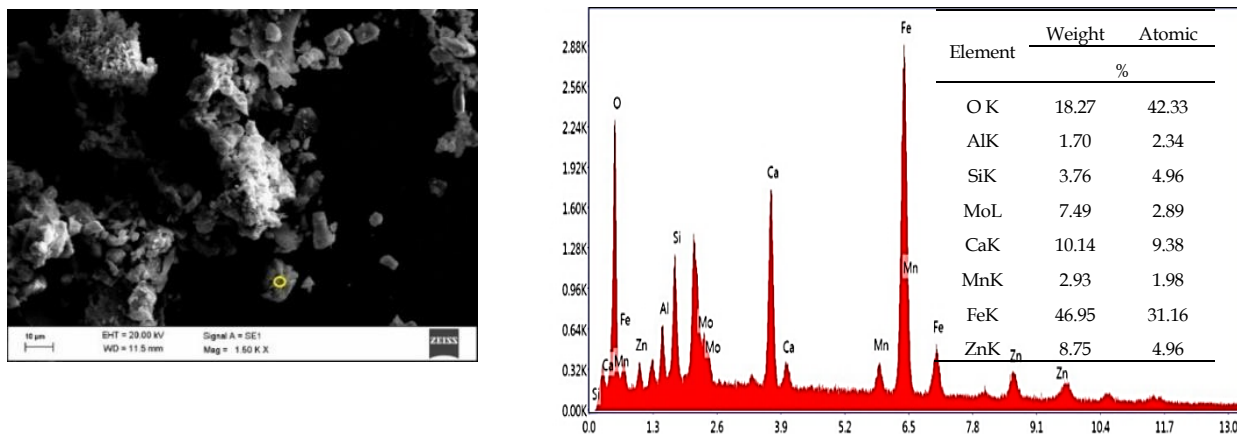| Element	Weight	Atomic
		%
O K	18.27	42.33
AlK	1.70	2.34
SiK	3.76	4.96
MoL	7.49	2.89
CaK	10.14	9.38
MnK	2.93	1.98
FeK	46.95	31.16
ZnK	8.75	4.96

Fig. 7. a) SEM analysis of the waste sample (left-fig.); b) EDX analysis of the marked area in the SEM image of the waste sample (right-fig.)

A black precipitate formed after 48 h in the Na_2S + NaOH leaching solution in the refractory gold ores containing antimony. Iron, sodium, sulfur, oxygen and antimony were also found in the SEM/EDX analysis conducted on this precipitated solid (Yang et al., 2017). Many elements such as iron, oxygen, calcium, zinc, molybdenum, manganese, silicon, and aluminum were also detected by EDX after leaching in this study.

3.2.4. XRD (X-ray diffraction) Rietveld's analysis

The XRD Rietveld's analysis of the raw material sample (Fig. 8) revealed quartz, dolomite, calcite, hematite, beudantite, hemimorphite, muscovite, smithsonite, goethite, and hydrozincite minerals. The most abundant of these minerals (Table 2) were goethite (22.0%), quartz (20.8%), calcite (20.0%), muscovite (16.3%), and dolomite (11.0%).

In comparison of the results of the XRD Rietveld's analysis of the post-pretreatment sample (Fig. 9) with the raw material sample, hematite, muscovite and hydrozincite minerals could not be detected.
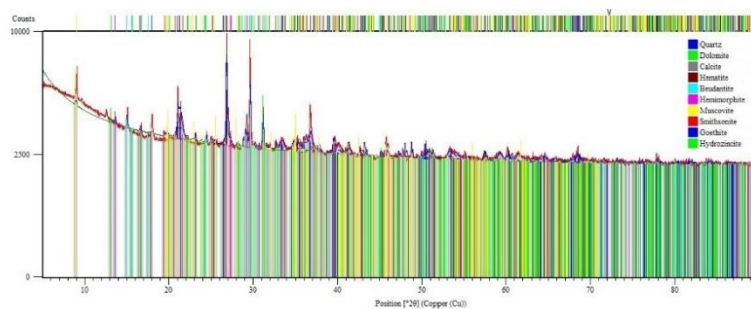

Fig. 8. XRD Rietveld's analysis of the raw material sample

However, vermiculite, kaolinite and plumbojarosite minerals were observed. The minerals with the highest content in the product (Table 2) were goethite (23.9%), quartz (21.0%), calcite (18.2%), kaolinite (15.2%), and dolomite (12.7%).

Contrary to the post-heat treatment sample, the XRD Rietveld's analysis of the waste sample (Fig. 10) revealed vermiculite and kaolinite minerals, as well as hematite, muscovite and hydrozincite minerals, while only plumbojarosite was not found like the raw material sample. As seen in Table 2, the content of the cyanidation test waste sample differed from the other two samples and the rate of the goethite mineral (9.3%) decreased. The other minerals of high-content were quartz (29.9%), calcite (23.5%), kaolinite (13.0%), and dolomite (12.4%).

In the XRD Rietveld's analysis of the microwave + leaching (NaCl + HCl) study on the Pb-containing phases, as a result of the experiments, the percentage content of Pb jarosite decreased,
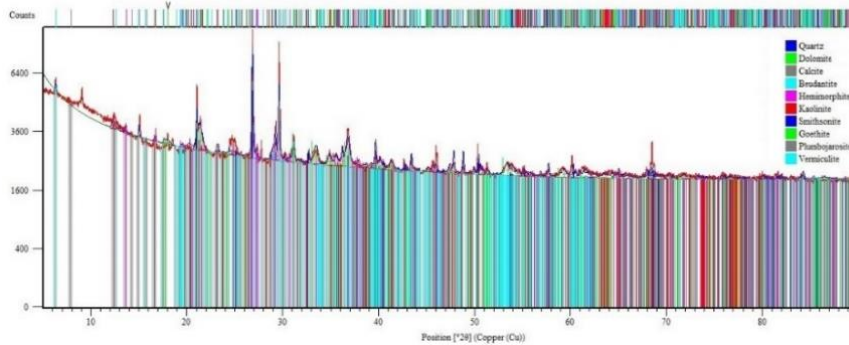

Fig. 9. XRD Rietveld's analysis of the product sample

Table 2. Percentage Mineral Content of XRD Rietveld's Analyses (RM: the raw material, P: the product, W: the waste)

| Mineral	Formula	RM	P	W
Quartz	SiO_2	20.8	21.0	29.9
Dolomite	$CaMg(CO_3)_2$	11.0	12.7	12.4
Calcite	$CaCO_3$	20.0	18.2	23.5
Hematite	Fe_2O_3	1.1	0.0	1.7
Beudantite	$PbFe_3(AsO_4)(SO_4)(OH)_6$	1.9	0.7	2.1
Hemimorphite	$Zn_4Si_2O_7(OH)_2 \cdot H_2O$	5.0	3.7	5.6
Muscovite	$KAl_2(AlSi_3O_{10})(OH)_2$	16.3	0.0	0.4
Kaolinite	$Al_2(Si_2O_5)(OH)_4$	0.0	15.2	13.0
Smithsonite	$ZnCO_3$	1.2	1.1	1.3
Goethite	$FeO(OH)$	22.00	23.9	9.3
Plumbojarosite	$(Pb(Fe_3(OH)_6(SO_4)_2)_2$	0.0	3.2	0.0
Hydrozincite	$Zn_5(CO_3)_2(OH)_6$	0.7	0.0	0.3
Vermiculite	$(Mg,Fe^{2+},Fe^{3+})_3[(Al,Si)_4O_{10}](OH)_2 \cdot 4H_2O$	0.0	0.3	0.5
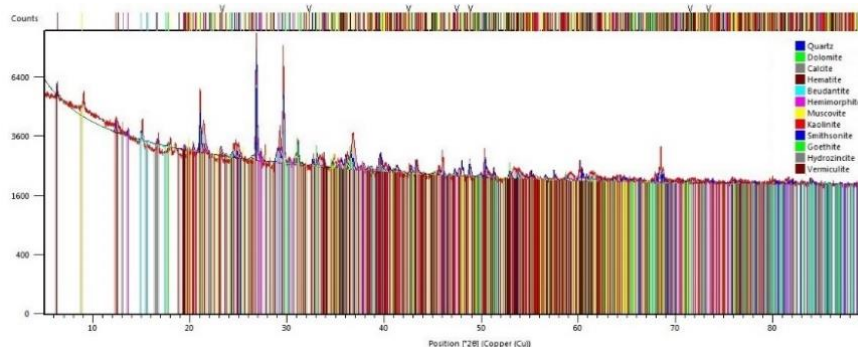
Fig. 10. XRD Rietveld's analysis of the waste sample

while the percentage content of structures such as anglesite $PbSO_4$ and $PbCl_2$ increased (Abo Atia and Spooren, 2020). In this study, calcite and quartz, which are gangue minerals, were observed to increase in abundance in the waste sample after the leaching process.

4. Conclusions

In this paper, cyanidation tests of oxidized refractory ores after microwave roasting were investigated. Characterization studies were carried out in terms of the mineral-element content of the ore, product, and waste samples. Gold and silver recovery rates ranged between 80 and 90% and 39 and 48%, respectively, in 24-hour cyanide tests after 6-minute pretreatment processes at different microwave powers. When the TG analysis of the samples in terms of mass changes was performed by thermal analysis, the losses were determined at 300, 600, and 1000°C, just as in the results of the degradation of the jarosite. Additionally, other compounds such as H_2O, O_2, CO_2, Fe_2O_3, and SO_4, where these valuable ingredients were found together or in inclusions, were decomposed by heat treatment. In particular, the high mass loss in the waste sample also affected the Au/Ag percentage recovery results with the effect of jarosite and other mineral degradations. According to the results of the FT-IR analysis, especially the percentage permeability of the waste sample increased. Since the ore had an oxidized and polymetallic structure, this change was likely to occur as a result of the clarification of minerals containing Pb, Zn, and Fe following all the processes. In the SEM/EDX analyzes, minerals such as carbonate and silicate, which were formed as a result of the degradation of the jarosite samples, were detected in the waste sample. Moreover, the Pb-Zn elements were also determined after heat treatment and in the waste sample. In the XRD Rietveld analysis, similar to other analyses, an increase in the concentrations of calcite, quartz, and kaolinite, and a decrease in the concentration of goethite minerals were detected, especially in the waste sample. This can be explained by the degradation of gangue minerals and the recovery of valuable content in the vicinity of Fe oxy/oxyhydroxide.

Acknowledgements

References

ABDOLMOHAMMAD-ZADEH, H., SALMASI, M.A., 2018. *A Nano-Composite Based on Fe3O4@Styrene-Maleic Anhydride Copolymer as a Magnetic Sorbent for Preconcentration of Silver(I) Ion*. Anal. Bioanal. Chem. Res. 5, 23–39. https://doi.org/10.22036/abcr.2017.88163.1147

ABO ATIA, T., SPOOREN, J., 2020. *Microwave assisted chloride leaching of zinc plant residues*. J. Hazard. Mater. 398, 122814. https://doi.org/10.1016/J.JHAZMAT.2020.122814

ACARKAN, N., BULUT, G., GÜL, A., KANGAL, O., KARAKAŞ, F., KÖKKILIÇ, O., ÖNAL, G., 2011. *The Effect of Collector's Type on Gold and Silver Flotation in a Complex Ore*. Sep. Sci. Technol. 46, 283–289. https://doi.org/10.1080/01496395.2010.512029

ADAMS, M.D., 2005. Advances in gold ore processing. Elsevier B.V.

AGBOZU, I., UWEM, B., NDOKIARI, B., 2017. *Uptake of Zn, Pb, Cu and Fe Ions from Spent and Unspent Engine Oil Using Termite Soil*. Int. J. Chem. 9, 85. https://doi.org/10.5539/ijc.v9n3p85

AGRAWAL, S., RAYAPUDI, V., DHAWAN, N., 2019. *Comparison of microwave and conventional carbothermal reduction of red mud for recovery of iron values*. Miner. Eng. 132, 202–210. https://doi.org/10.1016/j.mineng.2018.12.012

AI-YUAN, M., XUE-MEI, Z., JIN-HUI, P., LI-BO, Z., SRINIVASAKANNAN, C., LI, J., CHENG-LONG, W., 2017. *Dechlorination of zinc oxide dust derived from zinc leaching residue by microwave roasting in a rotary kiln*. Brazilian J. Chem. Eng. 34, 193–202. https://doi.org/10.1590/0104-6632.20160331s00003530

AL-HARAHSHEH, M., KINGMAN, S., BRADSHAW, S., 2006. *Scale up possibilities for microwave leaching of chalcopyrite in ferric sulphate*. Int. J. Miner. Process. 80, 198–204. https://doi.org/10.1016/j.minpro.2006.04.003

AMANKWAH, R.K., OFORI-SARPONG, G., 2011. *Microwave heating of gold ores for enhanced grindability and cyanide amenability.* Miner. Eng. 24, 541–544. https://doi.org/10.1016/j.mineng.2010.12.002

AYLMORE, M., JAFFER, A., 2012. *Evaluating process options for treating some refractory ores.* Proc. ALTA 2012 Gold Sess. 249–283.

BOBICKI, E.R., LIU, Q., XU, Z., 2014. *Microwave heating of ultramafic nickel ores and mineralogical effects.* Miner. Eng. 58, 22–25. https://doi.org/10.1016/j.mineng.2014.01.003

BURAT, F., BAŞTÜRKCÜ, H., ÖZER, M., 2019. *Gold&silver recovery from jewelry waste with combination of physical and physicochemical methods.* Waste Manag. 89, 10–20. https://doi.org/10.1016/j.wasman.2019.03.062

CAO, P., ZHANG, S., ZHENG, Y., LAI, S., LIANG, G., WANG, X., TAN, B., 2021. *Identification of elements hindering gold leaching from gold-bearing dust and selection of gold extraction process.* Hydrometallurgy 202, 105612. https://doi.org/10.1016/j.hydromet.2021.105612

CHOI, N.C., KIM, B.J., CHO, K., LEE, S., PARK, C.Y., 2017. *Microwave pretreatment for thiourea leaching for gold concentrate.* Metals (Basel). 7, 1–8. https://doi.org/10.3390/met7100404

CHUPROV, L.A., SENNIKOV, P.G., TOKHADZE, K.G., IGNATOV, S.K., SCHREMS, O., 2006. *High-resolution Fourier-transform IR spectroscopic determination of impurities in silicon tetrafluoride and silane prepared from it.* Inorg. Mater. 42, 924–931. https://doi.org/10.1134/S0020168506080231

CLARKSON, G., CLARKSON, R., HITCH, M., 2016. *Exploiting the malleability of gold for placer concentrate extraction and recovery.* Miner. Eng. 94, 38–40. https://doi.org/10.1016/j.mineng.2016.04.017

DE MICHELIS, I., OLIVIERI, A., UBALDINI, S., FERELLA, F., BEOLCHINI, F., VEGLIÒ, F., 2013. *Roasting and chlorine leaching of gold-bearing refractory concentrate: Experimental and process analysis.* Int. J. Min. Sci. Technol. 23, 709–715. https://doi.org/10.1016/j.ijmst.2013.08.015

DJOMGOUE, P., NJOPWOUO, D., 2013. FT-IR *Spectroscopy Applied for Surface Clays Characterization.* J. Surf. Eng. Mater. Adv. Technol. 03, 275–282. https://doi.org/10.4236/jsemat.2013.34037

DUNN, J.G., CHAMBERLAIN, A.C., 1997. T*he recovery of gold from refractory arsenopyrite concentrates by pyrolysis-oxidation.* Miner. Eng. 10, 919–928. https://doi.org/10.1016/s0892-6875(97)00074-5

EL-NAFATY, U., MUHAMMAD, I., ABDULSALAM, S., 2013. *Biosorption and Kinetic Studies on Oil Removal from Produced Water Using Banana Peel.* Civ. Environ. … 3, 125–136.

FARAJI, S., ANI, F.N., 2014. *Microwave-assisted synthesis of metal oxide/hydroxide composite electrodes for high power supercapacitors - A review.* J. Power Sources 263, 338–360. https://doi.org/10.1016/j.jpowsour.2014.03.144

FARAZ, S., HOSSNA, D., REZGAR, B., PIROZ, Z., 2014. *Improved recovery of a low-grade refractory gold ore using flotation-preoxidation-cyanidation methods.* Int. J. Min. Sci. Technol. 24, 537–542. https://doi.org/10.1016/j.ijmst.2014.05.018

FORSTER, J., MAHAM, Y., BOBICKI, E.R., 2018. *Microwave heating of magnesium silicate minerals.* Powder Technol. 339, 1–7. https://doi.org/10.1016/j.powtec.2018.07.069

FORSTER, J., PICKLES, C.A., ELLIOTT, R., 2016. *Microwave carbothermic reduction roasting of a low grade nickeliferous silicate laterite ore.* Miner. Eng. 88, 18–27. https://doi.org/10.1016/j.mineng.2015.09.005

FROST, R.L., PALMER, S.J., KRISTÓF, J., HORVÁTH, E., 2010. *Thermoanalytical studies of silver and lead jarosites and their solid solutions.* J. Therm. Anal. Calorim. 101, 73–79. https://doi.org/10.1007/s10973-009-0406-8

FROST, R.L., WILLS, R.A., WEIER, M.L., MUSUMECI, A.W., MARTENS, W., 2005. *Thermal decomposition of natural and synthetic plumbojarosites: Importance in 'archeochemistry.'* Thermochim. Acta 432, 30–35. https://doi.org/10.1016/J.TCA.2005.04.001

HAN, G., WEN, S., WANG, H., FENG, Q., 2021. *Sulfidization regulation of cuprite by pre-oxidation using sodium hypochlorite as an oxidant.* Int. J. Min. Sci. Technol. 31, 1117–1128. https://doi.org/10.1016/j.ijmst.2021.11.001

HAQUE, K.E., 1999. *Microwave energy for mineral treatment processes - A brief review.* Int. J. Miner. Process. 57, 1–24. https://doi.org/10.1016/s0301-7516(99)00009-5

HARTLIEB, P., TOIFL, M., KUCHAR, F., MEISELS, R., ANTRETTER, T., 2016. *Thermo-physical properties of selected hard rocks and their relation to microwave-assisted comminution.* Miner. Eng. 91, 34–41. https://doi.org/10.1016/j.mineng.2015.11.008

HASSANI, F., NEKOOVAGHT, P.M., GHARIB, N., 2016. *The influence of microwave irradiation on rocks for microwave-assisted underground excavation.* J. Rock Mech. Geotech. Eng. 8, 1–15. https://doi.org/10.1016/j.jrmge.2015.10.004

HOLMES, T., CRAIG, D., BATCHELOR, A.R., DODDS, C., KINGMAN, S.W., LEGAULT, E., WHETTON, M., 2020. Selective Heat Ore Treatment : Shaking Up The Economics of Mineral Recovery, in: Proceedings of COM2020 Conference of Metallurgists.

HUNT, J., FERRARI, A., LITA, A., CROSSWHITE, M., ASHLEY, B., STIEGMAN, A.E., 2013. *Microwave-Specific Enhancement of the Carbon − Carbon Dioxide (Boudouard) Reaction.* J. Phys. Chem. 117, 26871−26880. https://doi.org/doi.org/10.1021/jp4076965

IDRISS, H., LLORCA, J., 2019. *Low temperature infrared study of carbon monoxide adsorption on rh/ceo2* [WWW Document]. Catalysts. https://doi.org/10.3390/catal9070598

JABEEN, B., RAFIQUE, U., 2014. *Synthesis and application of metal doped silica particles for adsorptive desulphurization of fuels.* Environ. Eng. Res. 19, 205–214. https://doi.org/10.4491/eer.2014.017

JIA, X., YAO, Y., YU, G., QU, L., LI, T., LI, Z., XU, C., 2020. *Synthesis of gold-silver nanoalloys under microwave-assisted irradiation by deposition of silver on gold nanoclusters/triple helix glucan and antifungal activity.* Carbohydr. Polym. 238, 116169. https://doi.org/10.1016/j.carbpol.2020.116169

JONES, D.A., KINGMAN, S.W., WHITTLES, D.N., LOWNDES, I.S., 2005. *Understanding microwave assisted breakage.* Miner. Eng. 18, 659–669. https://doi.org/10.1016/j.mineng.2004.10.011

KASAINI, H., KASONGO, K., NAUDE, N., KATABUA, J., 2008. *Enhanced leachability of gold and silver in cyanide media: Effect of alkaline pre-treatment of jarosite minerals.* Miner. Eng. 21, 1075–1082. https://doi.org/10.1016/j.mineng.2007.12.005

KAUFFMAN, K.L., CULP, J.T., GOODMAN, A., MATRANGA, C., 2011. *FT-IR study of CO_2 adsorption in a dynamic copper(II) benzoate-pyrazine host with CO_2-CO_2 interactions in the adsorbed state.* J. Phys. Chem. C 115, 1857–1866. https://doi.org/10.1021/jp102273w

KAYA, M., HUSSAINI, S., KURSUNOGLU, S., 2020. *Critical review on secondary zinc resources and their recycling technologies.* Hydrometallurgy 195, 105362. https://doi.org/10.1016/j.hydromet.2020.105362

KIEFER, J., STRK, A., KIEFER, A.L., GLADE, H., 2018. *Infrared spectroscopic analysis of the inorganic deposits from water in domestic and technical heat exchangers.* Energies 11. https://doi.org/10.3390/en11040798

KINGMAN, S.W., ROWSON, N.A., 1998. *Microwave treatment of minerals - A review.* Miner. Eng. 11, 1081–1087. https://doi.org/10.1016/s0892-6875(98)00094-6

KLIMESCH, D.S., RAY, A., 1998. *DTA-TGA of unstirred autoclaved metakaolin-lime-quartz slurries. The formation of hydrogarnet.* Thermochim. Acta. https://doi.org/10.1016/S0040-6031(98)00307-4

KUMAR, S., RAJKUMAR, P., 2009. *Characterization of minerals in air dust particles in the state of Tamilnadu, India through FTIR Spectroscopy*, 1–17. doi.org/10.5194/acpd-13-22221-2013

LA BROOY, S.R., LINGE, H.G., WALKER, G.S., 1994. Review of gold extraction from ores. Miner. Eng. 7, 1213–1241. https://doi.org/10.1016/0892-6875(94)90114-7

LARRABURE, G., RODRÍGUEZ-REYES, J.C.F., 2021. *A review on the negative impact of different elements during cyanidation of gold and silver from refractory ores and strategies to optimize the leaching process.* Miner. Eng. 173, 107194. https://doi.org/10.1016/J.MINENG.2021.107194

LI, H., LONG, H., ZHANG, L., YIN, S., LI, S., ZHU, F., XIE, H., 2020. *Effectiveness of microwave-assisted thermal treatment in the extraction of gold in cyanide tailings.* J. Hazard. Mater. 384. https://doi.org/10.1016/j.jhazmat.2019.121456

LI, H., PENG, J., MA, P., ZHOU, Z., LONG, H., LI, S., ZHANG, L., 2021. *Application of diagnostic roasting method in thermochemical treatment for Au recovery from gold-containing tailings in microwave field.* Miner. Eng. 163, 106773. https://doi.org/10.1016/j.mineng.2021.106773

LI, Q., LI, D., QIAN, F., 2009. *Pre-oxidation of high-sulfur and high-arsenic refractory gold concentrate by ozone and ferric ions in acidic media.* Hydrometallurgy 97, 61–66. https://doi.org/10.1016/j.hydromet.2009.01.002

LIU, C., JU, S.H., ZHANG, L.B., SRINIVASAKANNAN, C., PENG, J.H., LE, T.Q.X., GUO, Z.Y., 2017. *Recovery of valuable metals from jarosite by sulphuric acid roasting using microwave and water leaching.* Can. Metall. Q. 56, 1–9. https://doi.org/10.1080/00084433.2016.1242972

LORENZO-TALLAFIGO, J., IGLESIAS-GONZÁLEZ, N., MAZUELOS, A., ROMERO, R., CARRANZA, F., 2019. *An alternative approach to recover lead, silver and gold from black gossan (polymetallic ore). Study of biological oxidation and lead recovery stages.* J. Clean. Prod. 207, 510–521. https://doi.org/10.1016/j.jclepro.2018.10.041

LU, G. MING, LI, Y. HUI, HASSANI, F., ZHANG, X., 2017. *The influence of microwave irradiation on thermal properties of main rock-forming minerals.* Appl. Therm. Eng. 112, 1523–1532. https://doi.org/10.1016/j.applthermaleng.2016.11.015

LUO, P., ZHAO, Y., ZHANG, B., LIU, JINDUN, YANG, Y., LIU, JUNFANG, 2010. *Study on the adsorption of Neutral Red from aqueous solution onto halloysite nanotubes.* Water Res. 44, 1489–1497. https://doi.org/10.1016/j.watres.2009.10.042

LUO, W., SI, Y., WANG, H., QIN, Y., HUANG, F., WANG, C., 2011. *Leather material found on a 6th B.C. Chinese bronze sword: A technical study.* Spectrochim. Acta - Part A Mol. Biomol. Spectrosc. 79, 1630–1633. https://doi.org/10.1016/j.saa.2011.05.023

LUNIN, V.D., NARSEEV, A. V., BARASHNEV, N.I., RATNIKOV, E. V., 1997. M*odel of Process of Microwave Action on Refractory Gold Concentrate.* J. Min. Sci. 33, 373–377.

MA, G., GARBERS-CRAIG, A.M., 2006. *A review on the characteristics, formation mechanisms and treatment processes of Cr (VI)-containing pyrometallurgical wastes.* J. South. African Inst. Min. Metall. 106, 753–763.

MESTA, B., ÖZTÜRK, A.O., EVIN, G., GÜMÜŞ, N., 2009. *Madenköy kompleks madenï (altin, gümüş , kurşun, çinko) proje tanitim dosyasi* (in Turkish). Ankara.

MILETTO, I., CATIZZONE, E., BONURA, G., IVALDI, C., MIGLIORI, M., GIANOTTI, E., MARCHESE, L., FRUSTERI, F., GIORDANO, G., 2018. *In situ FT-IR characterization of CuZnZr/ferrierite hybrid catalysts for one-pot CO2-to-DME conversion.* Materials (Basel). 11. https://doi.org/10.3390/ma11112275

MOGRE, P., GANACHARI, SHARANABASAVA V., YARADODDI, JAYACHANDRA S., BANAPURMATH, NAGARAJ N., HUNASHYAL, A.M., SHETTAR, A.S., 2018. *Synthesis and characterization studies of polyaniline nano fibres.* Adv. Mater. Proc. 3, 178–180. https://doi.org/10.5185/amp.2018/015

NANTHAKUMAR, B., PICKLES, C.A., KELEBEK, S., 2007. *Microwave pretreatment of a double refractory gold ore.* Miner. Eng. 20, 1109–1119. https://doi.org/10.1016/j.mineng.2007.04.003

OJIMA, J., 2003. *Determining of crystalline silica in respirable dust samples by Infrared Spectrophotometry in the presence of interferences.* J. Occup. Health 45, 94–103. https://doi.org/10.1539/joh.45.94

PARGA, J.R., VALENZUELA, J.L., DÍAZ, J.A., 2012. *New Technology for Recovery of Gold and Silver by Pressure Cyanidation Leaching and Electrocoagulation,* Noble Metals. https://doi.org/10.5772/32673

PENG, Z., HWANG, J.Y., 2015. *Microwave-assisted metallurgy.* Int. Mater. Rev. 60, 30–63. https://doi.org/10.1179/1743280414Y.0000000042

SANCHES, N.B., CASSU, S.N., DE CÁSSIA LAZZARINI DUTRA, R., 2015. *TG/FT-IR characterization of additives typically employed in EPDM formulations.* Polimeros 25, 247–255. https://doi.org/10.1590/0104-1428.1819

SBIHI, K., CHERIFI, O., BERTRAND, M., EL GHARMALI, A., 2014. *Biosorption of metals (Cd, Cu and Zn) by the freshwater diatom Planothidium lanceolatum: A laboratory study.* Diatom Res. 29, 55–63. https://doi.org/10.1080/0269249X.2013.872193

SCHMUHL, R., SMIT, J.T., MARSH, J.H., 2011. *The influence of microwave pre-treatment of the leach behaviour of disseminated sulphide ore.* Hydrometallurgy. https://doi.org/10.1016/j.hydromet.2011.04.001

SEFLEK, C., BAYAT, O., 2018. *Microwave-Assisted Grinding of Bolkardag (Nigde, Turkey) Gold Ore and Enhanced Cyanide Leachability.* Metall. Res. Technol. 115. https://doi.org/10.1051/metal/2018039

SHAHRAKI, B.K., MEHRABI, B., DABIRI, R., 2009. *Thermal behavior of Zefreh dolomite mine (Centeral Iran).* J. Min. Metall. Sect. B Metall. 45, 35–44. https://doi.org/10.2298/JMMB0901035S

SINADINOVIC, D., KAMBEROVIC, Z., VAKANJAC, B., 1999. *Refractory gold ores, characteristics and methods of their procession,* in: VIII Balkan Mineral Processing Conference. Yugoslavia, pp. 411–418.

SINHAMAHAPATRA, A., GIRI, A.K., PAL, P., PAHARI, S.K., BAJAJ, H.C., PANDA, A.B., 2012. *A rapid and green synthetic approach for hierarchically assembled porous ZnO nanoflakes with enhanced catalytic activity.* J. Mater. Chem. 22, 17227–17235. https://doi.org/10.1039/c2jm32998k

ŠONTEVSKA, V., JOVANOVSKI, G., MAKRESKI, P., RAŠKOVSKA, A., ŠOPTRAJANOV, B., 2008. *Minerals from Macedonia. XXI. Vibrational spectroscopy as identificational tool for some phyllosilicate minerals.* Acta Chim. Slov. 55, 757–766.

SUBHAN, M.A., SARKER, P., AHMED, T., 2014. A*nalysis of Kidney and Gall Stones of Patients from North-East Bangladesh by FTIR.* J. Sci. Res. 6, 553–561. https://doi.org/10.3329/jsr.v6i3.16721

TOIFL, M., HARTLIEB, P., MEISELS, R., ANTRETTER, T., KUCHAR, F., 2017. *Numerical study of the influence of irradiation parameters on the microwave-induced stresses in granite.* Miner. Eng. 103–104, 78–92. https://doi.org/10.1016/j.mineng.2016.09.011

VEIGA, M.M., GUNSON, A.J., 2020. *Gravity concentration in artisanal gold mining.* Minerals 10, 1–50. https://doi.org/10.3390/min10111026

VOLPI, M., PIROLA, C., ROTA, G., NÓBREGA, J.A., CARNAROGLIO, D., 2022. *Microwave-assisted sample preparation of a-spodumene: A simple procedure for analysis of a complex sample.* Miner. Eng. 187. https://doi.org/10.1016/j.mineng.2022.107820

WALKIEWICZ, J.W., KAZONICH, G., MCGILL, S. L., 1988. *Microwave heating characteristics of selected minerals and compounds.*

YANG, T., RAO, S., LIU, W., ZHANG, D., CHEN, L., 2017. *A selective process for extracting antimony from refractory gold ore.* Hydrometallurgy 169, 571–575. https://doi.org/10.1016/j.hydromet.2017.03.014

YOĞURTCUOĞLU, E., 2017. *Effect of Grinding and Alkali Pretreatment in Before Cyanidation of Oxidized Refractory Au/Ag Ores* (in Turkish), PhD thesis, Karadeniz Technical University, Trabzon, Turkey.

ZHANG, L., ZHU, Y., LI, D., WANG, M., CHENA, H., WUA, J., 2019. *Preparation and characterization of fully renewable polybenzoxazines from monomers containing multi-oxazine rings*. AIChE Annu. Meet. Conf. Proc. 2019-Novem. https://doi.org/10.1039/x0xx00000x

ZHAO, Q.H., ZHAO, X.B., ZHENG, Y.L., LI, J.C., HE, L., HE, J.L., ZOU, C.J., 2020. *Heating characteristics of igneous rock-forming minerals under microwave irradiation.* Int. J. Rock Mech. Min. Sci. 135, 1–6. https://doi.org/10.1016/j.ijrmms.2020.104519